

Solution conformation of a tetradecapeptide stabilized by two di-*n*-propyl glycine residues

Vijayalekshmi Sarojini,^{a,b*} R. Balaji Rao,^c S. Ragothama^d
and Padmanabhan Balaram^a

The solution conformation of a designed tetradecapeptide Boc-Val-Ala-Leu-Dpg-Val-Ala-Leu-Val-Ala-Leu-Dpg-Val-Ala-Leu-OMe (Dpg-14) containing two di-*n*-propyl glycine (Dpg) residues has been investigated by ¹H NMR and circular dichroism in organic solvents. The peptide aggregates formed at a concentration of 3 mM in the apolar solvent CDCl₃ were broken by the addition of 12% v/v of the more polar solvent DMSO-*d*₆. Successive N_{*i*}H ↔ N_{*i*+1}H NOEs observed over the entire length of the sequence in this solvent mixture together with the observation of several characteristic medium-range NOEs support a major population of continuous helical conformations for Dpg-14. Majority of the observed coupling constants (³J_{NHC^αH}) also support ϕ values in the helical conformation. Circular dichroism spectra recorded in methanol and propan-2-ol give further support in favor of helical conformation for Dpg-14 and the stability of the helix at higher temperature. Copyright © 2010 European Peptide Society and John Wiley & Sons, Ltd.

Keywords: di-*n*-propyl glycine; nuclear Overhauser effect; helical conformation; tetradecapeptide

Introduction

The intrinsic conformational flexibility of short peptides can be overcome by incorporating C^{α,α}-di-*n*-alkylglycines in designed peptides judiciously. The ability of C^{α,α}-di-*n*-alkylglycines to promote specific secondary structures in designed peptides is well documented in literature for the prototype residue Aib and its higher homologues with linear (Dxg) as well as cycloalkyl [1-amino cycloalkane 1-carboxylic acid (Ac_{*n*}C)] side chains [1–10]. Based on theoretical calculations, helical conformations are lower in energy than fully extended conformations for the prototype residue Aib and Ac_{*n*}C, whereas fully extended conformations are marginally lower in energy than helical conformations for dialkylglycines with linear alkyl chains (Dxg) [1,5,11]. Nevertheless, peptide helices containing α,α-di-*n*-propyl glycine (Dpg) and α,α-di-*n*-butylglycine residues have been reported experimentally in the solid state [12,13]. In solution, peptide helices containing Dxg amino acids have been shown to be more susceptible to solvent- and temperature-induced conformational transitions in comparison to peptide helices containing Aib and Ac_{*n*}C amino acids [10]. Limited studies have been carried out on peptide helices where helix folding is dictated by amino acids in the Dxg category alone. We present here solution conformational analysis on the longest Dpg-containing peptide helix, reported so far, without any Aib residues. NMR results demonstrate that the peptide folds into a helical conformation, stabilized by two properly positioned Dpg residues. Circular dichroism studies provide evidence for the stability of the **Dpg-14** helix at temperatures as high as 80 °C. The solution conformation of **Dpg-14** reported in this paper is in perfect agreement with its crystal structure reported by us elsewhere [14].

Materials and Methods

Peptide Synthesis

Dpg was synthesized by procedures reported elsewhere [15]. The peptide was synthesized by conventional solution-phase procedures using a fragment condensation strategy. The Boc group was used for *N*-terminal protection and the C-terminus was protected as a methyl ester (OMe). *N*- and C-terminal deprotections were performed using 98% formic acid or saponification, respectively. Coupling reactions for the preparation of dipeptides were mediated by DCC in DCM and all other couplings were carried out in DMF, in the presence of DCC and HOBt. All the intermediate peptides were characterized by ¹H NMR (80 MHz) and TLC and used without further purification. The final peptide was purified by medium pressure liquid chromatography on a reversed-phase C₁₈ column (40–60 μm) followed by HPLC on a C₁₈ column (4 × 250-mm particle size 5–10 μm) using methanol–water gradients. Homogeneity of the purified peptide was established by HPLC. The final peptide was fully characterized by 500-MHz

* Correspondence to: Vijayalekshmi Sarojini, Department of Chemistry, University of Auckland, Private Bag 92019, Auckland, New Zealand.
E-mail: v.sarojini@auckland.ac.nz

a Molecular Biophysics Unit, Indian Institute of Science, Bangalore-560012, India

b Department of Chemistry, University of Auckland, Private Bag 92019, Auckland, New Zealand

c Department of Chemistry, Banaras Hindu University, Varanasi-221005, India

d Sophisticated Instruments Facility, Indian Institute of Science, Bangalore-5600121, India

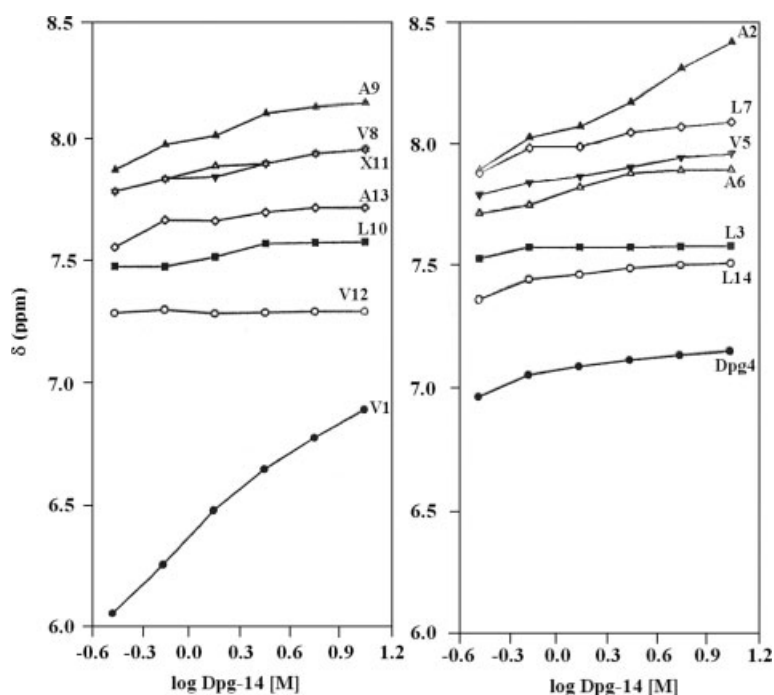


Figure 1. Concentration dependence of NH chemical shifts for **Dpg-14** in CDCl_3 [$X = \text{Dpg}$].

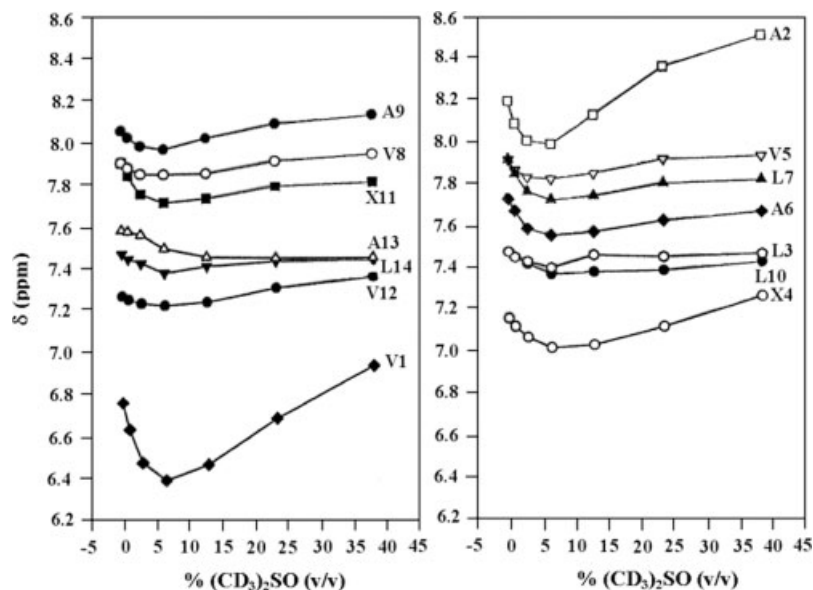


Figure 2. Solvent dependence of NH chemical shifts for **Dpg-14** in CDCl_3 - $(\text{CD}_3)_2\text{SO}$ mixtures at varying composition [$X = \text{Dpg}$].

^1H NMR and ESI mass spectrometry, $[\text{M} + \text{Na}]^+_{\text{obs}}$ 1571 Da, M_{calcd} = 1548 Da.

Spectroscopic Studies

All NMR experiments were carried out on Bruker AMX-400 and DRX-500 spectrometers at the Sophisticated Instrumentation Facility, Indian Institute of Science, Bangalore. All NMR spectra were recorded at a peptide concentration of 3 mM. Two-dimensional (2D) data were acquired at 1 K data points, 512 experiments, with 48–64 transients. A 300-ms mixing time was used for ROESY experiments. The spectral width for

all the experiments was set to 4500 Hz. Nuclear magnetic resonance data were processed using XWINNMR software. All 2D data sets were zero filled to 1024 points with a 90° phase-shifted squared sine-bell filter in both dimensions. The probe temperature was maintained at 300 K. CD spectra were recorded on a JASCO J-500 spectropolarimeter equipped with a DP-501 data processor using a 1-mm path length cell. Temperature-dependent CD spectra were recorded using a thermostated cell holder. Samples were equilibrated for 10 min at every temperature before recording the spectra. CD band intensities are expressed as molar ellipticities $[\theta]_{\text{M}}$ in degree $\text{cm}^2 \text{dmol}^{-1}$.

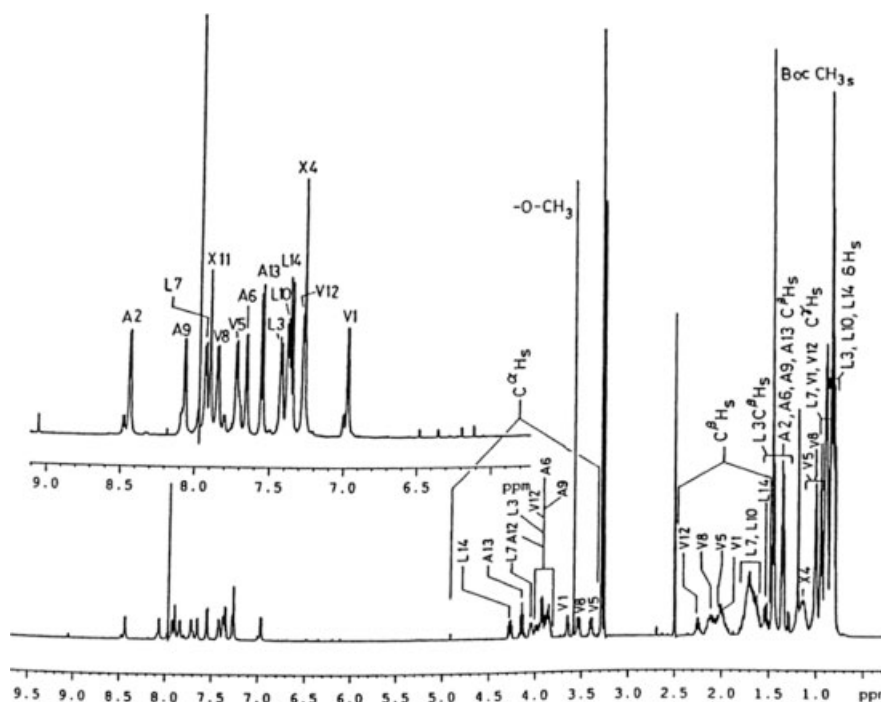


Figure 3. 500-MHz ^1H NMR spectrum of **Dpg-14** in 88% CDCl_3 and 12% $(\text{CD}_3)_2\text{SO}$ [$X = \text{Dpg}$].

Table 1. NMR parameters for **Dpg-14** in CDCl_3 : DMSO-d_6 (88 : 12)

Residue	Chemical shifts					$^3\text{J}_{\text{NH}^{\alpha}\text{H}}$
	NH	C^{α}	C^{β}	C^{γ}	C^{δ}	
Val (1)	6.97	3.95	2.0	0.91	–	4.0
Ala (2)	8.43	3.93	1.35	–	–	4.2
Leu (3)	7.42	3.91	1.69	1.41	0.84	6.2
Dpg (4)	7.27	–	2.13, 1.97	1.57	–	–
Val (5)	7.72	3.57	2.0	0.98	–	4.5
Ala (6)	7.65	3.91	1.42	–	–	4.0
Leu (7)	7.93	4.04	1.68	1.42	0.85	5.3
Val (8)	7.84	3.53	2.07	1.0	–	5.4
Ala (9)	8.06	3.85	1.37	–	–	3.6
Leu (10)	7.37	3.84	1.52	–	0.82	5.2
Dpg (11)	7.89	–	2.10	–	–	–
Val (12)	7.28	3.92	2.23	0.93	–	4.7
Ala (13)	7.55	4.14	1.37	–	–	7.7
Leu (14)	7.35	4.27	1.53	1.31	0.80	7.7

Results and Discussion

NMR Assignments

Sequence-specific ^1H NMR assignments were readily achieved for **Dpg-14** using a combination of 2D TOCSY and ROESY experiments. Proton chemical shifts and coupling constants obtained for **Dpg-14** in the solvent mixture CDCl_3 : $(\text{CD}_3)_2\text{SO}$ (88 : 12) are summarized in Table 1.

1D NMR

The ^1H NMR spectrum of **Dpg-14** at 3 mM concentration recorded in CDCl_3 showed broad peaks suggesting aggregation in this

solvent. Peptide aggregation is further verified in the solvent and concentration dependence of NH chemical shifts which are described below. However, addition of up to 12% (v/v) of DMSO-d_6 to the peptide solution in CDCl_3 resulted in sharp peaks suggesting the breaking up of the peptide aggregates.

Concentration Dependence of NH Chemical Shifts

Figure 1 shows the variation of NH chemical shifts as a function of peptide concentration in CDCl_3 over the range 10–0.3 mM. Concentration dependence is most pronounced for Val (1) and Ala (2) with the NH groups of these two residues moving sharply downfield over the range studied. This is possibly because of the formation of peptide aggregates involving these two NH groups. The chemical shifts of the remaining 12 NH groups do not show significant concentration dependence in this solvent.

Delineation of Solvent-Shielded NH Groups

Figure 2 shows the effect of addition of a hydrogen-bonding solvent DMSO to a solution of the peptide in an apolar solvent CDCl_3 . Normally, addition of small amounts of DMSO results in monotonic downfield shifts of solvent-exposed NH groups in peptides, whereas solvent-shielded NH groups remain largely unaffected [16,17]. Results obtained in the case of **Dpg-14** are striking with several NH groups showing anomalous pattern. The NH groups of Val (1) and Ala (2) move upfield up to a DMSO concentration of ~5% (v/v). Above 5% DMSO, these resonances move considerably downfield with saturation being observed at ~40% (v/v) of DMSO. The NH groups of residues Leu (3) to Leu (14) remain largely unperturbed to changes in solvent polarity. This shows that NH groups of residues from Leu (3) to Leu (14) in the sequence are involved

in intramolecular hydrogen bonds and thus remain shielded from the solvent. However, the strong dependence of chemical shifts of Val (1) and Ala (2) NH groups to changes in solvent polarity indicate the solvent-exposed nature of these two residues. The solvent-exposed nature of Val (1) and Ala (2) NH groups in the apolar solvent CDCl₃ facilitates their involvement in intermolecular hydrogen bonds resulting in the formation of peptide aggregates. The polar solvent DMSO competes for hydrogen bonding with these NH groups breaking the peptide aggregates at 5% (v/v) of DMSO. Further increase in the concentration of DMSO results in more pronounced downfield shifts of Val (1) and Ala (2) NH groups, whereas the NH groups of the residues 3–14 remain largely unperturbed confirming their involvement in intramolecular hydrogen bonding. Synthetic fragments of membrane channel-forming polypeptides, alamethicin and suzukacillin have been shown to form aggregates in aqueous and nonaqueous media [18–20].

Nuclear Overhauser Effects

The ¹H NMR spectrum of **Dpg-14** at a DMSO concentration of 12% (v/v), a concentration which is not expected to result in major structural perturbations in the molecule, showed all resonances as sharp well-dispersed peaks (Figure 3). NOEs for **Dpg-14** determined in this solvent mixture showed strong sequential N_iH ↔ N_{i+1}H NOES over the entire length of the peptide, whereas the corresponding C_i^αH ↔ N_{i+1}H NOES were either absent or very weak. Observation of a series of N_iH ↔ N_{i+1}H (d_{NN}) NOEs and the absence of strong C_i^αH ↔ N_{i+1}H (d_{αN}) NOEs clearly indicate that **Dpg-14** exists predominantly as a helix under these conditions. Helical conformation in peptides also brings into proximity backbone protons of residues that are not adjacent in the sequence. Thus, NOEs of the type C_i^αH ↔ N_{i+2}H, C_i^αH ↔ N_{i+3}H and C_i^αH ↔ N_{i+4}H could also be observed in peptide helices. In ideal 3₁₀ and α-helical conformations, the d_{αN}(i, i + 2), d_{αN}(i, i + 3) and d_{αN}(i, i + 4) distances are 3.8, 3.3 and 4.5 Å (3₁₀ helix) and 4.4, 3.4 and 4.2 Å (α-helix). Figure 4 shows an expansion of the C^αH ↔ NH region of the ROESY spectrum of **Dpg-14** in the solvent mixture 88% CDCl₃ and 12% DMSO-d₆ which clearly shows the presence of weak NOEs between V (1) C^αH ↔ L (3) NH, A (6) C^αH ↔ V (8) NH, L (7) C^αH ↔ A (9) NH and V (8) C^αH ↔ L (10) NH, all of which fall in the d_{αN}(i, i + 2) category. Also observed are V (1) C^αH ↔ Dpg (4) NH, V (5) C^αH ↔ V (8) NH and V (8) C^αH ↔ Dpg (11) NH belonging to the d_{αN}(i, i + 3) category and finally a weak NOE between V (5) C^αH ↔ A (9) NH which corresponds to the d_{αN}(i, i + 4) interaction. Figure 5 shows the expansion of the C^αH ↔ C^βH region of the ROESY spectrum. The presence of two NOEs of medium intensity, namely A (2) C^αH ↔ V (5) C^βH and A (9) C^αH ↔ V (12) C^βH, are noteworthy. These NOEs arise out of d_{αβ}(i, i + 3) interactions. The d_{αβ}(i, i + 3) distance for an ideal α-helix is 2.5–4.4 Å, which is within the NOE observable distance. The NOEs observed in **Dpg-14** are summarized in Figure 6. Coupling constants of **Dpg-14** listed in Table 1 illustrate that with the exception of A (13) and L (14) NH resonances, all other NH groups have J values <6.5 Hz characteristic of φ values in the helical conformation.

Conformation of **Dpg-14** in CDCl₃: (CD₃)₂SO (88 : 12)

An examination of the chemical shift dependence of NH resonances of **Dpg-14** in CDCl₃/(CD₃)₂SO mixtures suggests that

Table 2. Medium-range NOEs characteristic of helical conformations observed in **Dpg-14**

NOEs observed in Dpg-14		Typical NOE observable distance (Å)	
Type	Residue position	3 ₁₀ -Helix	α-Helix
α-N _{i,i+2}	V(1)-L(3)	3.8	4.4
	A(6)-V(8)		
	L(7)-A(9)		
	V(8)-L(10)		
α-N _{i,i+3}	V(1)-Dpg(4)	3.3	3.4
	V(5)-V(8)		
	V(8)-Dpg(11)		
α-N _{i,i+4}	V(5)-A(9)		4.2
α-β _{i,i+3}	A(2)-V(5)	3.1–5.1	2.5–4.4
	A(9)-V(12)		

the aggregates formed by intermolecular hydrogen bonding involving Val (1) and Ala (2) NH groups in the apolar solvent CDCl₃ are broken at a DMSO concentration of >5%. This is due to the ability of DMSO to compete for hydrogen bonding to NH groups. The concentration and solvent dependence of NH chemical shifts in **Dpg-14**, taken together, indicate that all except Val (1) and Ala (2) NH groups in **Dpg-14** are involved in intramolecular hydrogen bonding. This is characteristic of helical conformations in peptides. ROESY spectra in CDCl₃/(CD₃)₂SO mixtures show all strong sequential d_{NN} connectivities. The d_{αN} connectivities are comparatively weak or absent. Observation of a series of N_iH to N_{i+1}H (d_{NN}) NOEs and the absence of intense C_i^αH to N_{i+1}H (d_{αN}) NOEs clearly indicate the existence of predominantly helical conformations in peptides. Several other nonsequential NOEs of the α-N and α-β categories (Table 2), characteristic of helical conformations, are also present in **Dpg-14** which strongly suggest that **Dpg-14** folds into a stable helix in the solvent system used. The observed coupling constant values are <6.5 Hz, except of Ala (13) and Leu (14). These values are suggestive of φ values in the helical conformation. The NMR results thus establish that largely helical conformations are maintained for **Dpg-14** in CDCl₃/(CD₃)₂SO mixtures (88 : 12).

Circular Dichroism Studies

CD spectra of **Dpg-14** were recorded in methanol and propan-2-ol. The CD spectra in the two solvents were identical in nature, but of varying intensity. The spectra in both solvents showed a negative shoulder at ~222 nm with deep minima at ~208 nm characteristic of helical peptides of similar length. Stability of the peptide helix was investigated as a function of temperature by circular dichroism spectroscopy. Figure 7 shows the CD spectra of **Dpg-14** in propan-2-ol as a function of temperature. The ratio [θ]₂₂₂/[θ]₂₀₈ which is a measure of helicity decreases from 0.67 at 20 °C to 0.55 at 80 °C. Even at 80 °C, **Dpg-14** has considerable helical structure which is evident from the CD spectrum at this temperature. For an ideal α-helix, the [θ]₂₂₂/[θ]₂₀₈ ratio has been predicted to be 1. For a 3₁₀-helix, the ratio [θ]₂₂₂/[θ]₂₀₈ is ~0.5 [21–23]. The ratio [θ]₂₂₂/[θ]₂₀₈ **Dpg-14** ranges from 0.67 to 0.55 at the temperature studied. This can be attributed to considerable amount of 3₁₀-helical structure of **Dpg-14**. Thus, results from the temperature-dependent CD studies show that the helical structure adopted by **Dpg-14** at

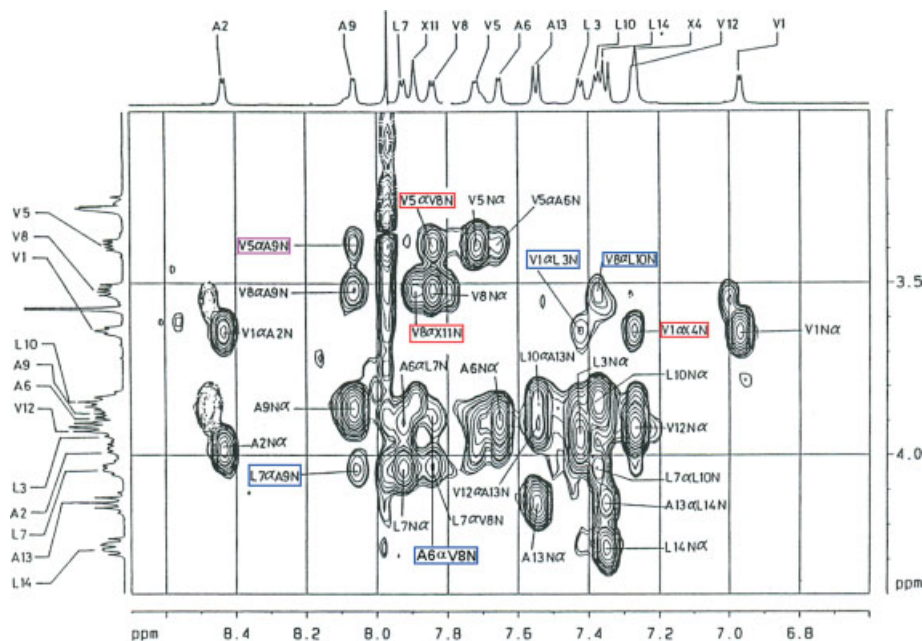


Figure 4. Partial 500-MHz ROESY spectrum of **Dpg-14** in 88% CDCl₃ and 12% (CD₃)₂SO showing C^αH ↔ NH NOEs.

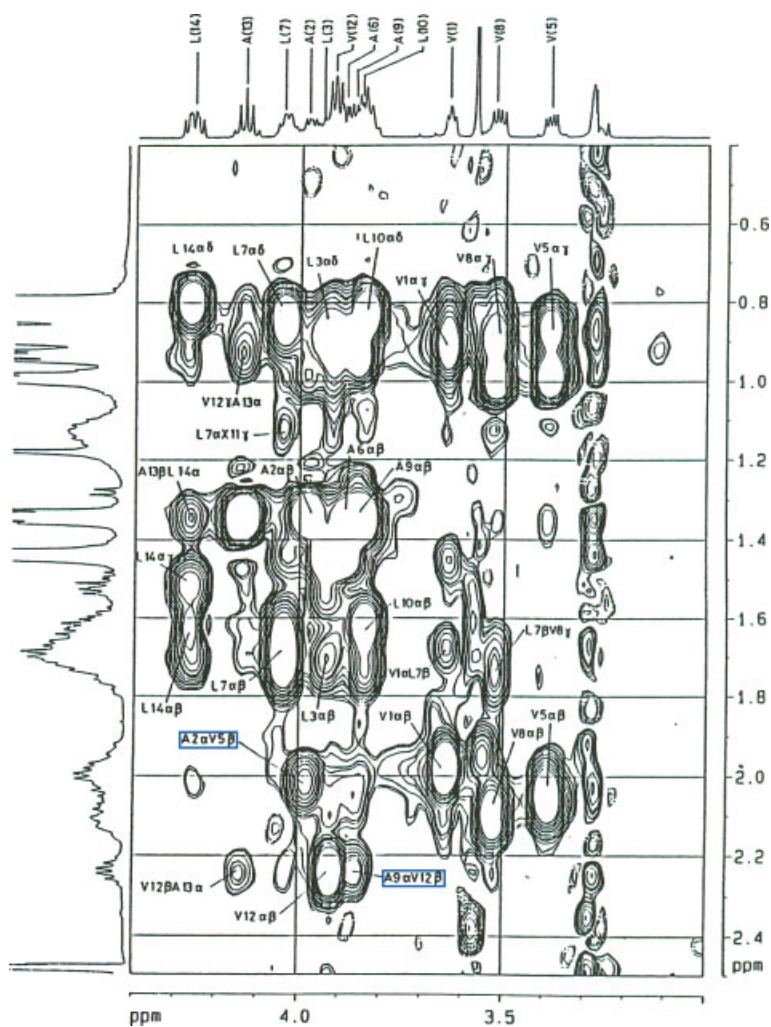


Figure 5. Partial 500-MHz ROESY spectrum of **Dpg-14** in 88% CDCl₃ and 12% (CD₃)₂SO showing C^αH ↔ C^βH NOEs [X = Dpg].

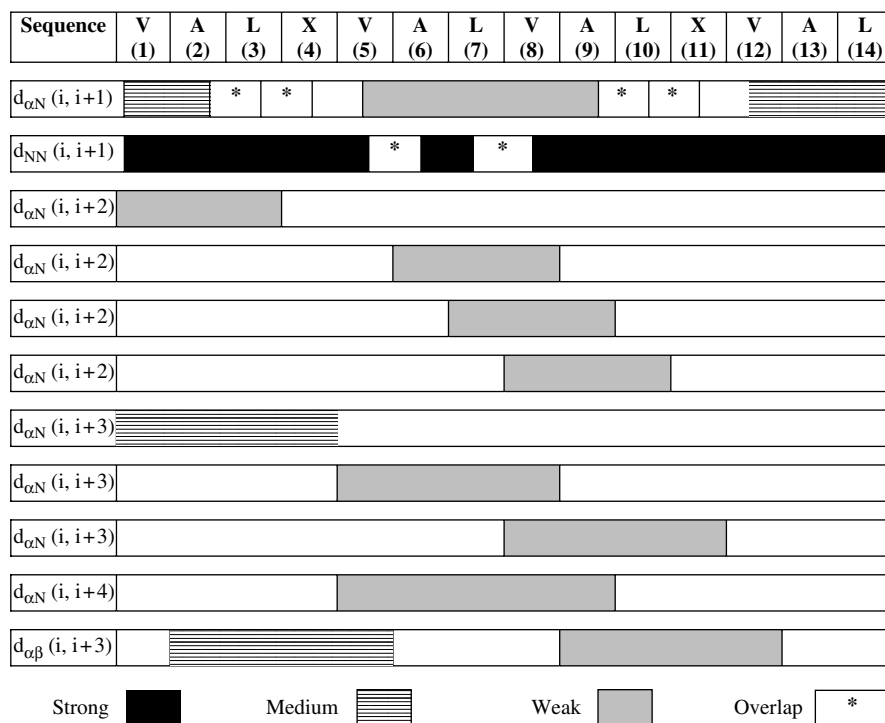


Figure 6. NOE summary for **Dpg-14** in 88% $CDCl_3$ and 12% $(CD_3)_2SO$. Peptide sequence is shown on top. NOE intensities are categorized as either strong, medium or weak and marked accordingly by different shades.

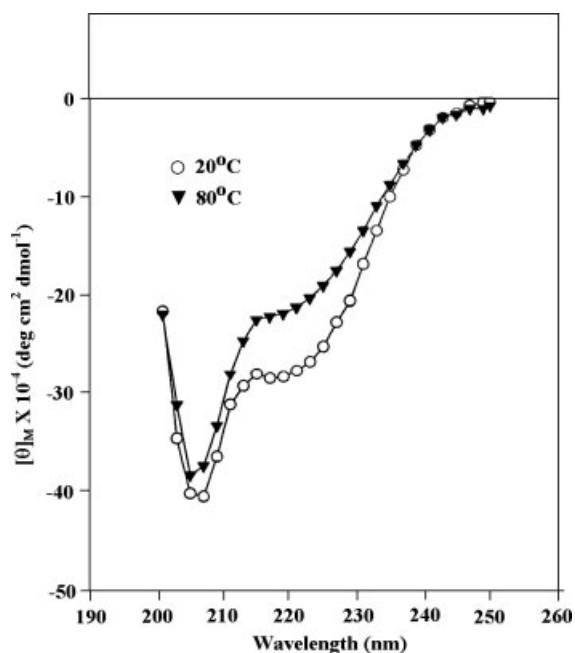


Figure 7. CD spectra of **Dpg-14** in 2-propanol at 20 and 80 °C.

room temperature remains largely unperturbed even at the higher temperature 80 °C.

Conclusions

Conformational energy calculations in the case of acyclic $C^{\alpha,\alpha}$ -dialkyl glycines (Deg, Dpg) have shown that the extended

conformation is energetically preferred over the helical conformation. However, studies on **Dpg-14** presented in this paper show unambiguously that for the Dpg residue exclusively helical conformations can be obtained by a proper choice of the sequence. **Dpg-14**, reported here, is longest Dpg-containing peptide helix without any Aib residues reported so far.

Acknowledgements

This research was supported by the Department of Science and Technology, Government of India. NMR spectra were recorded at the Sophisticated Instrumentation Facility, Indian Institute of Science, Bangalore, India.

References

- Prasad BVV, Balam P. The stereochemistry of peptides containing α -aminoisobutyric acid. *CRC Crit. Rev. Biochem.* 1984; **16**: 307–347.
- Balam P. The design and construction of synthetic protein mimics. *Pure Appl. Chem.* 1992; **64**: 1061–1066.
- Karle IL, Balam P. Structural characteristics of α -Helical peptide molecules containing Aib residues. *Biochemistry* 1990; **29**: 6747–6756.
- Karle IL, Flippen-Anderson JL, Sukumar M, Uma K, Balam P. Modular design of synthetic protein mimics. Crystal structure of two seven-residue helical peptide segments linked by ϵ -aminocaproic acid. *J. Am. Chem. Soc.* 1991; **113**: 3952–3956.
- Paul PKC, Sukumar M, Bardi R, Piazzesi AM, Valle G, Toniolo C, Balam P. Stereochemically constrained peptides. Theoretical and experimental studies on the conformations of peptides containing 1-aminocyclohexanecarboxylic acid. *J. Am. Chem. Soc.* 1986; **108**: 6363–6370.
- Bardi R, Piazzesi AM, Toniolo C, Sukumar M, Balam P. Stereochemistry of peptides containing 1-aminocyclopentanecarboxylic acid (Acc⁵): solution and solid-state conformations of Boc-Acc⁵-Acc⁵-NHMe. *Biopolymers* 1986; **25**: 1635–1644.

- 7 Valle G, Crisma M, Toniolo C, Prasad S, Rao RB, Sukumar M, Balam P. Stereochemistry of peptides containing 1-aminocycloheptane-1-carboxylic acid (Ac7c). Crystal structures of model peptides. *Int. J. Pept. Protein Res.* 1991; **38**: 511–518.
- 8 Datta S, Rathore RNS, Vijayalakshmi S, Vasudev PG, Rao RB, Balam P, Shamala N. Peptide helices with pendant cycloalkane rings. Characterization of conformations of 1-aminocyclooctane-1-carboxylic acid (Ac8c) residues in peptides. *J. Pept. Sci.* 2004; **10**: 160–172.
- 9 Karle IL, Rao RB, Prasad S, Kaul R, Balam P. Nonstandard amino acids in conformational design of peptides. Helical structures in crystals of 5–10 residue peptides containing dipropylglycine and dibutylglycine. *J. Am. Chem. Soc.* 1994; **116**: 10355–10361.
- 10 Vijayalakshmi S, Rao RB, Karle IL, Balam P. Comparison of helix-stabilizing effects of alpha, alpha-dialkyl glycines with linear and cycloalkyl side chains. *Biopolymers* 2000; **53**: 84–98.
- 11 Barone V, Leij F, Bavoso A, Di Blasio B, Grimaldi P, Pavone V, Pedone C. Conformational behavior of α, α -dialkylated peptides. *Biopolymers* 1985; **24**: 1759–1767.
- 12 Karle IL, Rao RB, Prasad S, Kaul R, Balam P. Nonstandard amino acids in conformational design of peptides. Helical structures in crystals of 5–10 residue peptides containing dipropylglycine and dibutylglycine. *J. Am. Chem. Soc.* 1994; **116**: 10355–10361.
- 13 Karle IL, Gurunath R, Prasad S, Kaul R, Rao RB, Balam P. Peptide design. Structural evaluation of potential nonhelical segments attached to helical modules. *J. Am. Chem. Soc.* 1995; **117**: 9632–9637.
- 14 Hegde RP, Aravinda S, Rai R, Kaul R, Vijayalakshmi S, Rao RB, Shamala N, Balam P. Conformation of di-n-propylglycine residues (Dpg) in peptides: crystal structures of a type I β -turn forming tetrapeptide and an α -helical tetradecapeptide. *J. Pept. Sci.* 2008; **14**: 648–659.
- 15 Prasad S, Rao RB, Balam P. Contrasting solution conformations of peptides containing α, α -dialkylated residues with linear and cyclic side chains. *Biopolymers* 1995; **35**: 11–20.
- 16 Pitner TL, Urry DW. Proton magnetic resonance studies in trifluoroethanol solvent mixtures as a means of delineating peptide protons. *J. Am. Chem. Soc.* 1972; **94**: 1399–1400.
- 17 Raj PA, Balam P. Conformational effects on peptide aggregation in organic solvents: spectroscopic studies of two chemotactic tripeptide analogs. *Biopolymers* 1985; **24**: 1131–1146.
- 18 Mathew MK, Nagaraj R, Balam P. Membrane channel-forming polypeptides. *J. Biol. Chem.* 1982; **257**: 2170–2176.
- 19 Iqbal M, Balam P. Membrane channel-forming polypeptides. 270-MHz proton magnetic resonance studies of the aggregation of the 11–21 fragment of suzukacillin in organic solvents. *Biochemistry* 1981; **20**: 7278–7284.
- 20 Iqbal M, Balam P. Aggregation of apolar peptides in organic solvents. Concentration dependence of $^1\text{H-NMR}$ parameters for peptide NH groups in 310 helical decapeptide fragment of suzukacillin. *Biopolymers* 1982; **21**: 1427–1433.
- 21 Manning M, Woody RW. Theoretical CD studies of polypeptide helices: Examination of important electronic and geometric factors. *Biopolymers* 1991; **31**: 569–586.
- 22 Woody RW. Circular Dichroism of Peptides. In *The Peptides: Conformation in Biology and Drug Design*, Vol. 5, Hruby VJ (ed.). Academic Press: Orlando, FL, 1985; 15–114.
- 23 Sudha TS, Vijayakumar EKS, Balam P. *Int. J. Pept. Protein Res.* 1983; **22**: 464–468.